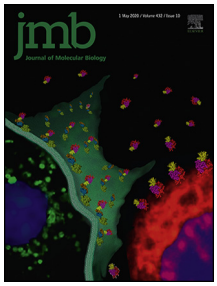

Ski Is Required for Tri-Methylation of H3K9 in Major Satellite and for Repression of Pericentromeric Genes: *Mmp3*, *Mmp10* and *Mmp13*, in Mouse Fibroblasts

Claudio Cappelli[1,6], Hugo Sepulveda[2], Solange Rivas[1], Víctor Pola[1], Ulises Urzúa[1], Gerardo Donoso[1], Eduardo Sagredo[1,5], David Carrero[1], Emmanuel Casanova-Ortiz[1], Alfredo Sagredo[1], Marisel González[1], Marcia Manterola[3], Gino Nardocci[2,4], Ricardo Armisén[1,5], Martin Montecino[2,4] and Katherine Marcelain[1]

1 - Departamento de Oncología Básico Clínica. Facultad de Medicina, *Universidad de Chile, Santiago, Chile*
2 - Instituto de Ciencias Biomédicas, *Facultad de Medicina y Facultad de Ciencias de la Vida, Universidad Andres Bello, Santiago, Chile*
3 - Instituto de Ciencias Biomédicas. Facultad de Medicina, *Universidad de Chile, Santiago, Chile*
4 - FONDAP Center for Genome Regulation, *Santiago, Chile*
5 - Centro de Genética y Genómica, *Instituto de Ciencias e Innovación en Medicina, Facultad de Medicina Clínica Alemana Universidad del Desarrollo, Santiago, Chile*
6 - Instituto de Bioquimica y Microbiologia, *Facultad de Ciencias, Universidad Austral de Chile, Valdivia, Chile.*

Correspondence to Katherine Marcelain: *Av. Independencia 1027, Block D, 3er piso, Independencia, Santiago, Chile.*
kmarcelain@med.uchile.cl
https://doi.org/10.1016/j.jmb.2020.03.013
Edited by M Yaniv

Abstract

Several mechanisms directing a rapid transcriptional reactivation of genes immediately after mitosis have been described. However, little is known about the maintenance of repressive signals during mitosis. In this work, we address the role of Ski in the repression of gene expression during M/G_1 transition in mouse embryonic fibroblasts (MEFs). We found that Ski localises as a distinct pair of dots at the pericentromeric region of mitotic chromosomes, and the absence of the protein is related to high acetylation and low tri-methylation of H3K9 in pericentromeric major satellite. Moreover, differential expression assays in early G_1 cells showed that the presence of Ski is significantly associated with repression of genes localised nearby to pericentromeric DNA. In mitotic cells, chromatin immunoprecipitation assays confirmed the association of Ski to major satellite and the promoters of the most repressed genes: Mmp3, Mmp10 and Mmp13. These genes are at pericentromeric region of chromosome 9. In these promoters, the presence of Ski resulted in increased H3K9 tri-methylation levels. This Ski-dependent regulation is also observed during interphase. Consequently, Mmp activity is augmented in Ski−/− MEFs. Altogether, these data indicate that association of Ski with the pericentromeric region of chromosomes during mitosis is required to maintain the silencing bookmarks of underlying chromatin.

Introduction

During mitosis, chromatin condenses to allow an even distribution of the genome in both daughter cells [1]. Chromosome condensation leads to the removal of the transcription machinery from chromatin, resulting in transcription termination [2–5] of most but not all genes [6,7].

The mechanism of re-establishment of the proper transcriptional program after mitosis in daughter cells is still unknown [8]. Prior studies have shown that a subset of transcription factors and transcriptional regulators are kept in mitotic chromosomes [9–16] to maintain the local epigenetic modifications, such as DNA methylation [17] and histones modifications [18–25], in order to re-establish an

inherited transcription program from mother to daughter cells.

This process, known as mitotic bookmarking, is mainly attributed to transcription factors such as GATA1 [12], FoxA1 [13] and Esrrb [14], which focally bind to chromatin during mitosis to favour immediate gene transcription in early G_1 phase. The mechanism by which bookmarking factors regulate early activation of specific genes after mitosis has been the focus of several investigations [12–14,19] [26]. Although it is crucial to re-establish gene expression patterns following mitosis, it is equally important to retain the repression of selected genes after this phase. However, how silencing of specific genes is maintained after chromosomes decondensation is poorly understood [11,27].

Ski is predominantly a nuclear protein forming part of transcriptional co-repressor complexes [28–31]. The transcriptional silencing activity associated with Ski was initially proposed by Nicol and Stavnezer in 1998 [32] and confirmed after the characterisation of a Ski-containing histone deacetylase complex (HDAC) [33], which is necessary for the transcriptional repression mediated by RB transcriptional corepressor 1 (Rb), Mad and thyroid hormone receptor [33,34]. In the same year, two independent groups demonstrated that Ski mediates the repression of TGF-β-dependent gene expression by recruiting the HDAC containing nuclear co-repressor complex to activated Smad protein in the nucleus [35–38]. The inhibition of gene expression activated by TGF-β signalling is so far the best-characterised mechanism of action of this protein [39–41]. In addition to TGF-β/Smad, Ski mediates the repressive activity of MeCP2 [42], Gli3 [43], GATA 1 [44], RAR-α [45,46] and RUNX1 [47]. In addition to its role in transcriptional regulation, it has also been suggested that Ski plays a role in mitosis, as it localises to centrosomes and the mitotic spindle in U2OS, Cos-1, Hela and HPV16-infected human keratinocytes (HK/HPV16) cells [48,49]. In mitosis, the levels of Ski increase [48,50], and it is phosphorylated by AURK-A [51] and cdc2/cdk1 [48]. Importantly, the absence of Ski in mouse embryonic fibroblasts (MEFs) results in a delayed mitotic onset, lagging chromosomes and micronuclei, and subsequent aneuploidy [52], suggesting that Ski is necessary to regulate critical events of this phase of the cell cycle. However, the specific role of Ski in mitosis is still unclear.

In this work, we show that Ski stays attached to the pericentromeric regions of mitotic chromosomes. This localisation of Ski is required for full tri-methylation of H3K9 and repression of genes at early G_1 phase of the cell cycle. In particular, Ski is required for repression of a cluster of 3 matrix metallopeptidase (*Mmp*) genes: 3, 10 and 13, located at the pericentromeric region of chromosome 9.

Altogether, our results indicate that the Ski co-repressor participates in a mechanism of maintenance of silencing of specific genes during mitosis.

Results

Ski associates with pericentromeric chromatin of mitotic chromosomes in MEFs

Previously, it has been shown that Ski knockout MEFs ($Ski^{-/-}$ MEFs) have several mitotic defects, such as a weakened spindle assembly checkpoint and chromosome segregation errors [52]. In order to understand the participation of Ski in the mitotic process, we analysed the localisation of the protein in mitotic MEFs by indirect immunofluorescence (IIF) and confocal microscopy. In $Ski^{-/-}$ MEFs, the expression of Ski was restored through the incorporation of the human Ski (SKI) homologue under control of a Tet-off promoter ($Ski^{-/-}$ + SKI MEFs). Using these models, we found that Ski localises to mitotic chromosomes appearing as a pair of dots close to but outside the centromere (Figure 1(a)). In order to attain a clearer view of Ski localisation in the chromosomes, IIF was performed on metaphase spreads. These experiments confirmed the localisation of Ski as a pair of dots on both sister chromatids, close to the centromeres, in a limited number of chromosomes (Figure 1(b) and Supplementary Figure 1A). The punctuated localisation pattern of Ski next to centromeres was also detected in immortalised wild-type (WT) MEFs, NIH3T3 and primary MEFs, while no signal was detected in $Ski^{-/-}$ MEFs (Supplementary Figure 1B–E). The same pattern was found in $Ski^{-/-}$ MEFs and NIH3T3 cells expressing a GFP-Ski protein (Figure 1(c) and Supplementary Figure 1F).

Most metaphases had eight chromosomes positive for the Ski signal. Still, this number was variable between metaphases, ranging from 8 to 19 per plate, with an average of 12 ± 3. As $Ski^{-/-}$ MEFs display a high degree of polyploidy [52], the presence of the protein was also quantified in primary MEFs, in order to have a more accurate result regarding the number of chromosomes positive for the protein. These cells also showed a variable but narrow number of chromosomes positive for Ski, ranging from 2 to 8, with most cells having four positive chromosomes per metaphase (Supplementary Figure 1C).

In mouse chromosomes, centromeric and pericentromeric satellite repeats are the minor (MiSat) and major (MaSat) satellites, respectively. A schematic representation of MiSat and MaSat localisation in a murine chromosome is shown in Figure 1(d). We

confirmed the association of Ski with the pericentromeric DNA through a chromatin immunoprecipitation (ChIP) assay. Ski was immunoprecipitated, and MaSat DNA was detected by qPCR (Figure 1(e)). In contrast, Ski was not found associated with centromeric MiSat DNA (Figure 1(f)).

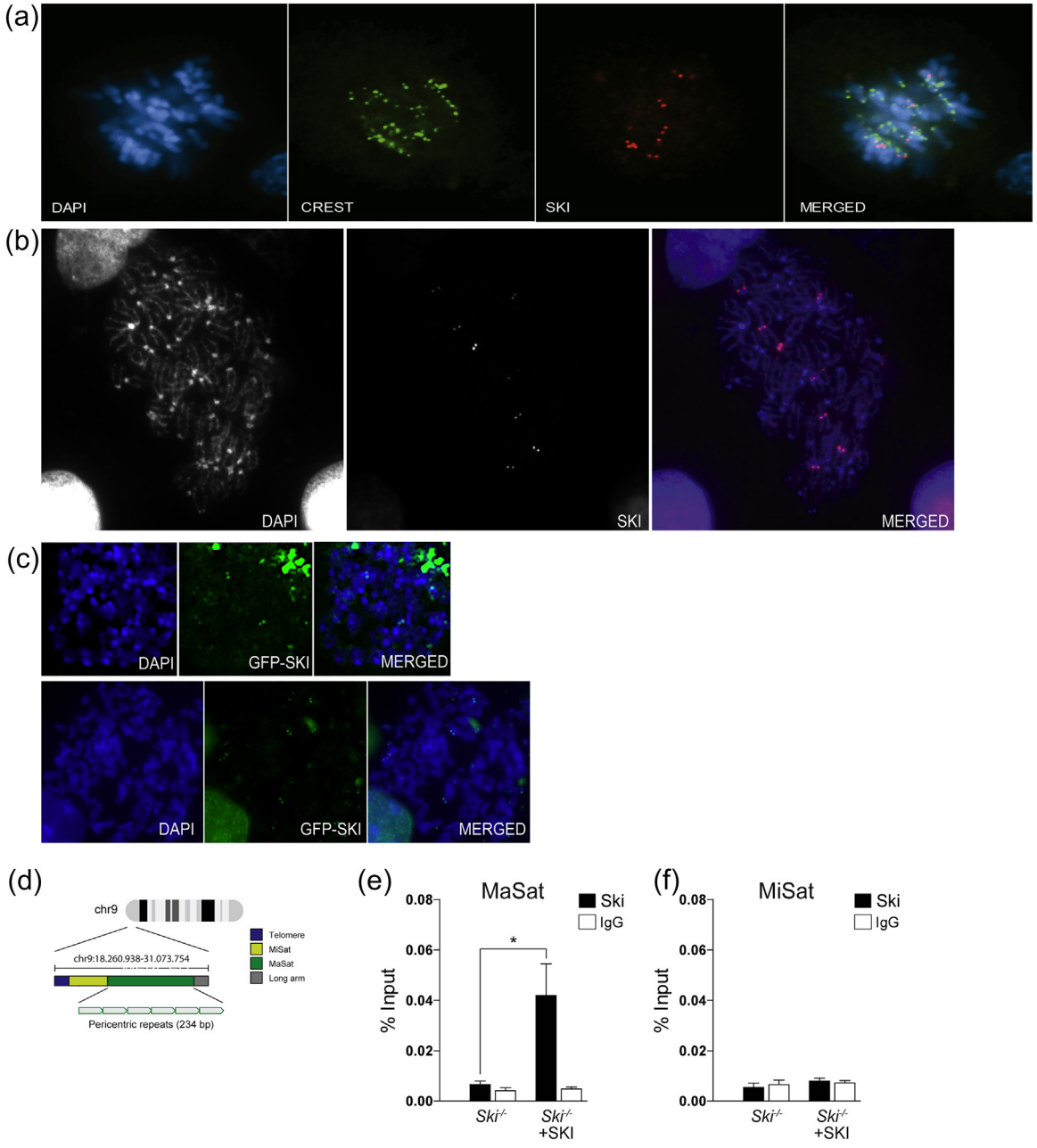

Figure 1. Ski associates with the pericentromeric region of mitotic chromosomes. Association of Ski to pericentromeric regions was evaluated by IIF and ChIP-qPCR in Ski$^{-/-}$ + SKI MEFs. (a) CREST (green) and Ski (red) were detected by IIF, using specific antibodies. DNA was stained with DAPI. A representative mitotic cell (z-stacks projection) is shown. (b) IIF was performed on metaphase spreads. (c) *Upper panel*: Ski was detected in mitotic MEFs stably expressing a GFP-Ski protein (after retroviral transduction). The fusion protein was detected by direct immunofluorescence using a 488-conjugated anti-GFP antibody. *Bottom panel*: GFP-Ski was detected in mitotic chromosomes of NIH-3 T3 cells transfected with a pCMV-GFP-Ski plasmid. The fusion protein was detected directly, without fixing the cells. (d) Schematic representation of analysed Satellite regions in a murine chromosome. (e) Ski was detected through a ChIP-qPCR assay on MaSat DNA in mitotic Ski$^{-/-}$ + SKI MEFs, but not on MiSat (f). Ski$^{-/-}$ MEFs were used as controls. % of Input is shown; unspecific IgG was used as a negative control. *$p < .05$; two-tailed *t*-test.

The absence of Ski is associated with increased H3K9 acetylation and decreased H3K9me3 of pericentromeric chromatin

Ski is known to be part of HDAC containing transcriptional co-repressor complexes [34,53]. Thus, we examined whether the presence of Ski on chromosomes was related to their histone acetylation status. Immunofluorescence on chromosomal spreads of Ski $^{-/-}$ + SKI MEFs showed that Ski does not co-localise with histone 3 Lys9 acetylation (H3K9ac) signals (Figure 2 (a) and (b)). Moreover, regions that were positive for Ski staining (Ski+) had lower H3K9ac signals when compared with equivalent regions in chromosomes negative for Ski staining (Ski–) (Figure 2(c)).

These data suggest that the presence of Ski could be affecting the modifications of H3K9 at pericentromeric regions. Thus, H3K9ac and H3K9me3

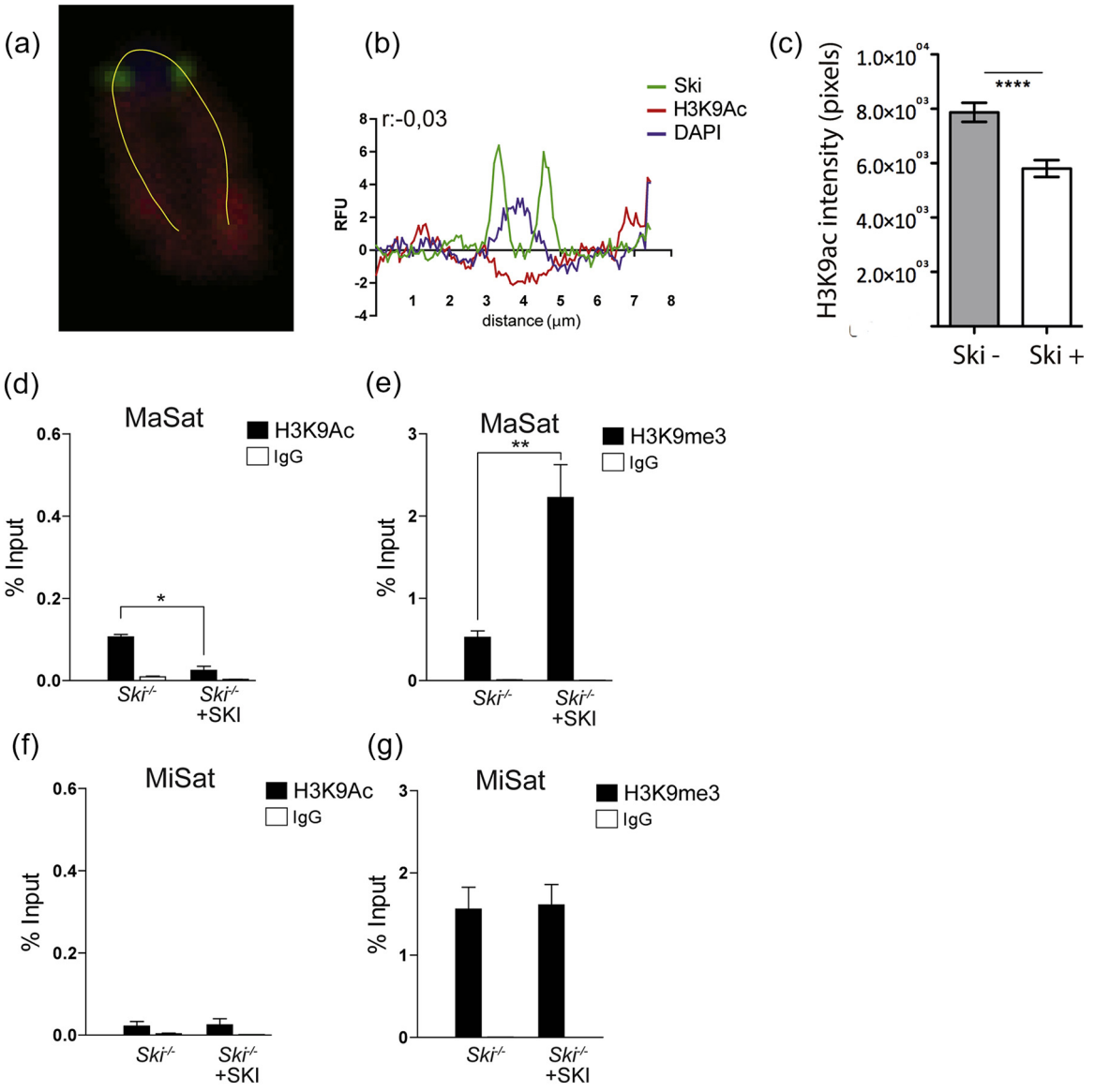

Figure 2. The presence of Ski is related to lower H3K9ac and higher H3K9me3 levels in pericentromeric regions of mitotic chromosomes. (a) Ski and H3K9ac were detected by IIF in metaphase spreads of Ski$^{-/-}$ + SKI and Ski$^{-/-}$ MEFs. A representative confocal Z stack of one chromosome stained for Ski (green) and H3K9ac (red) is shown. (b) Quantification of the relative fluorescence of each signal along the yellow line. *R*-value indicates the Pearson's correlation factor between Ski and H3K9ac signals. (c) Quantification of the relative fluorescence of H3K9ac in pericentromeric regions containing Ski and in equivalent regions of chromosomes negative for Ski staining. H3K9ac (d) and H3K9me3 (e) levels were quantified by ChIP-qPCR in MaSat chromatin of mitotic Ski$^{-/-}$ + SKI and Ski$^{-/-}$ MEFs. H3K9ac (f) and H3K9me3 (g) levels were quantified by ChIP-qPCR in MiSat chromatin of mitotic Ski$^{-/-}$ + SKI and Ski$^{-/-}$ MEFs. In d–g, % of Input is shown, and unspecific IgG was used as a negative control. *$p < .05$, **$p < .01$ and ****$p < .0001$; two-tailed *t*-test.

levels were quantified by ChIP-qPCR. In $Ski^{-/-}$ MEFs, the H3K9ac levels at pericentromeric MaSat chromatin were significantly higher than in $Ski^{-/-}$ + SKI MEFs (Figure 2(d)). In contrast, the levels of H3K9 tri-methylation (H3K9me3), a distinctive epigenetic mark of pericentromeric chromatin [23], were decreased in the MaSat of $Ski^{-/-}$ MEFs (Figure 2(e)).

As a control, H3K9me3 and H3K9ac levels were evaluated in MiSat. As expected, these regions were negative for H3K9ac marks; and the absence of Ski had no significant effect on H3K9me3 levels (Figure 2(f) and (g)).

The association of Ski with MaSat repeats and the effect of the absence of the protein on H3K9ac/me3 levels are preserved during interphase (Supplementary Figure 2A and B).

As mitotic chromosomes are highly condensed, we hypothesised that the effect of the absence of Ski on H3K9ac/me3 status in the MaSat chromatin

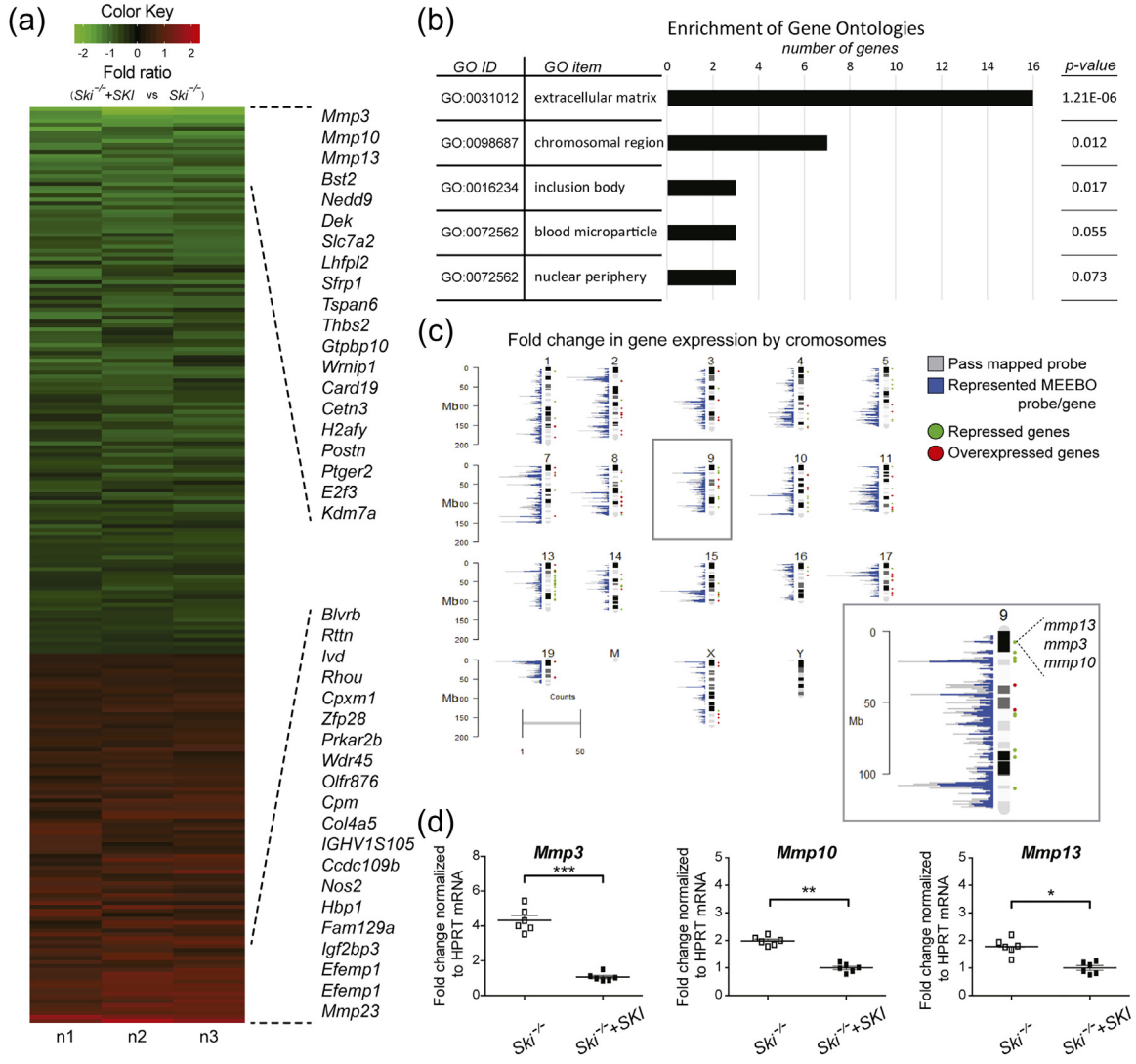

Figure 3. Ski-dependent differential gene expression at early G_1. $Ski^{-/-}$ + SKI and $Ski^{-/-}$ MEFs were cultured without Dox for 72 h and synchronised at early G_1 phase of the cell cycle. Differential gene expression was assessed by a cDNA-based array MEEBO. (a) Heat map of differentially expressed genes, in Ski expressing MEFs, compared to knockout cells. Top 20 repressed (green) and overexpressed (red) genes are indicated. Data from three independent experiments are shown. (b) Gene Ontology of differentially expressed genes. (c) Chromplot assignment of the repressed and overexpressed protein-coding genes along the entire mouse genome. Total MEEBO probes (blue) and the filter-passing probes (grey) are shown. No significant bias was found for filtered probes. Localisation of repressed (green) and overexpressed (red) genes are shown. Although filtered probes are evenly distributed, repressed genes are not. Inbox: Magnification of chromosome 9, the pericentromeric localisation of the three most repressed genes *Mmp* 3, 10 and 13 is indicated. (d) Validation of microarray results by RT-qPCR of the *Mmp* 3, 10 and 13 in MEFs synchronised at early G_1. $^*p < .05$, $^{**}p < .01$ and $^{***}p < .001$; two-tailed *t*-test.

would also extend to nearby areas. In those areas, the absence of Ski would affect the expression of underlying genes after resumption of transcription at the M-G_1 transition.

The presence of Ski is related to repression of genes nearby the pericentromeric region of chromosomes, during the early G_1 phase of the cell cycle

We evaluated whether the presence of Ski in the pericentromeric region of mitotic chromosomes was related to gene expression pattern at the early G_1 phase of the cell cycle. As we were unable to identify the specific chromosomes that contain Ski during mitosis, we used a genome-wide approach to identify the genes whose expression was affected by the presence of Ski in early G_1. Thus, $Ski^{-/-}$ and $Ski^{-/-}$ + SKI MEFs were synchronised at early G_1 (Supplementary Figure 3A and B), and differential gene expression was evaluated by MEEBO microarray platform (MEEBO, or Mouse Exonic Evidence-Based Oligonucleotides). After data processing and filtering, the array coverage decreased from approximately 30,300 probes to 12,340 robustly analysable probes, which corresponded to 8942 unique genes. The results of differential gene expression in $Ski^{-/-}$ and $Ski^{-/-}$ + SKI MEFs are shown in Figure 3(a). During early G_1, 139 genes are repressed, and 98 are overexpressed in $Ski^{-/-}$ + SKI MEFs compared to $Ski^{-/-}$ MEFs. The top 20 repressed and overexpressed genes are shown in Figure 3(a). A complete list of differentially expressed genes is available as Supplementary Material.

Gene Ontology pathway analysis [54] showed that the main biological processes or cellular component affected by the presence of Ski were extracellular matrix (ECM)-related functions, followed by chromosomal region and inclusion bodies (Figure 3(b)).

Using chromplot [55], we found that the chromosomal distribution of selected probes had no bias (Figure 3(c)), with a homogenous coverage of probes through all mouse chromosomes. However, further analysis of whole microarray data using the WebGestalt [56] platform indicated that the genes repressed upon expression of Ski are significantly associated with chromosome 13 and the region A of chromosome 9 ($p = 4.3 \times 10^{-8}$ and $p = .0024$, respectively; Table 1). In contrast, overexpressed genes are randomly distributed throughout the chromosomes.

Metalloproteinase activity, collagen catabolism and negative regulation of ossification were processes significantly repressed by Ski, and this repression was significantly associated with chromosome location (Table 2). Consistently, the three most repressed genes in Ski-expressing cells were *Mmp 13, Mmp 3 and Mmp 10*, all located in region A of chromosome 9 (inset in Figure 3(c)).

Table 1. Chromosomal distribution of genes repressed in $Ski^{-/-}$ + Ski MEFs at early G_1

Gene location	Chromosome	p^*
Whole chromosomes	Chr 13	3.3×10^{-10}
	Chr 9A	.0037
	Chr 14	.007
First 50 Mb	Chr 13	4.32×10^{-8}
	Chr 9A	.0027
First 20 Mb	Chr 9A	.0024

* *P* values according to cytogenetic band locator in the WebGestalt platform.

RT-qPCR assays validated microarray results for *Mmp* 13, *Mmp* 3 and *Mmp* 10 (Figure 3(d)) as well as for Dek, Nedd9, E2F3 and Elmo1 genes (Supplementary Figure 3D and E). To rule out a non-specific effect of the mitotic synchronisation protocol, *Mmp* 3 expression was also evaluated in early G_1 cells obtained after two additional protocols of mitotic synchronisation: by double thymidine block and nocodazole release (instead of colcemid); and by mitotic shake-off in the absence of depolymerizing drugs. There were no differences in the results (Supplementary Figure 3F and G).

Ski associates to *Mmp13, Mmp3 and Mmp10* gene promoters and its presence is required for tri-methylation of H3K9, in mitosis and interphase

In order to relate the effect of Ski on gene expression at early G_1 with its localisation in mitotic chromosomes, we assessed the presence of Ski at the promoter of *Mmp 3*, *Mmp 10* and *Mmp 13* genes in mitotic cells. ChIP assays were performed using primers designed to amplify the proximal promoter region of the *Mmp* 13 gene and flanking a putative Smad binding element (SBE) on *Mmp* 3 and *Mmp* 10 promoters (Figure 4(a)). As a control, ChIP assay was performed in mitotic $Ski^{-/-}$ MEFs. In these cells, the

Table 2. Altered pathways related to the chromosomal position

Chromosome location	Gene Ontology	
	Process	*p*
Whole chromosome	Mmp activity	.0144
	N.R.O.	.0181
First 50 Mb	N.R.O.	.0023
	C.C.	.0023
First 20 Mb	C.C.	.0002
	Mmp activity	.0011

N.R.O., negative regulator of ossification; C.C., collagen catabolism.

level of Ski antibody immunoprecipitating at the *Mmp* gene promoters was comparable to the negative control (normal IgG) (Figure 4(b), left). However, in mitotic Ski$^{-/-}$ + SKI MEFs, Ski occupies the proximal promoters of the three *Mmp* genes investigated (Figure 4(b), right). The relative enrichment of Ski at *Mmp* gene promoters was estimated using *the Gapdh* promoter as an internal control region. Enrichment of Ski at the promoters of the *Mmp* 3, *Mmp* 10 and *Mmp* 13 genes during mitosis is approximately four times higher in Ski-expressing MEFs compared to the Ski$^{-/-}$ MEFs (Figure 4(c)).

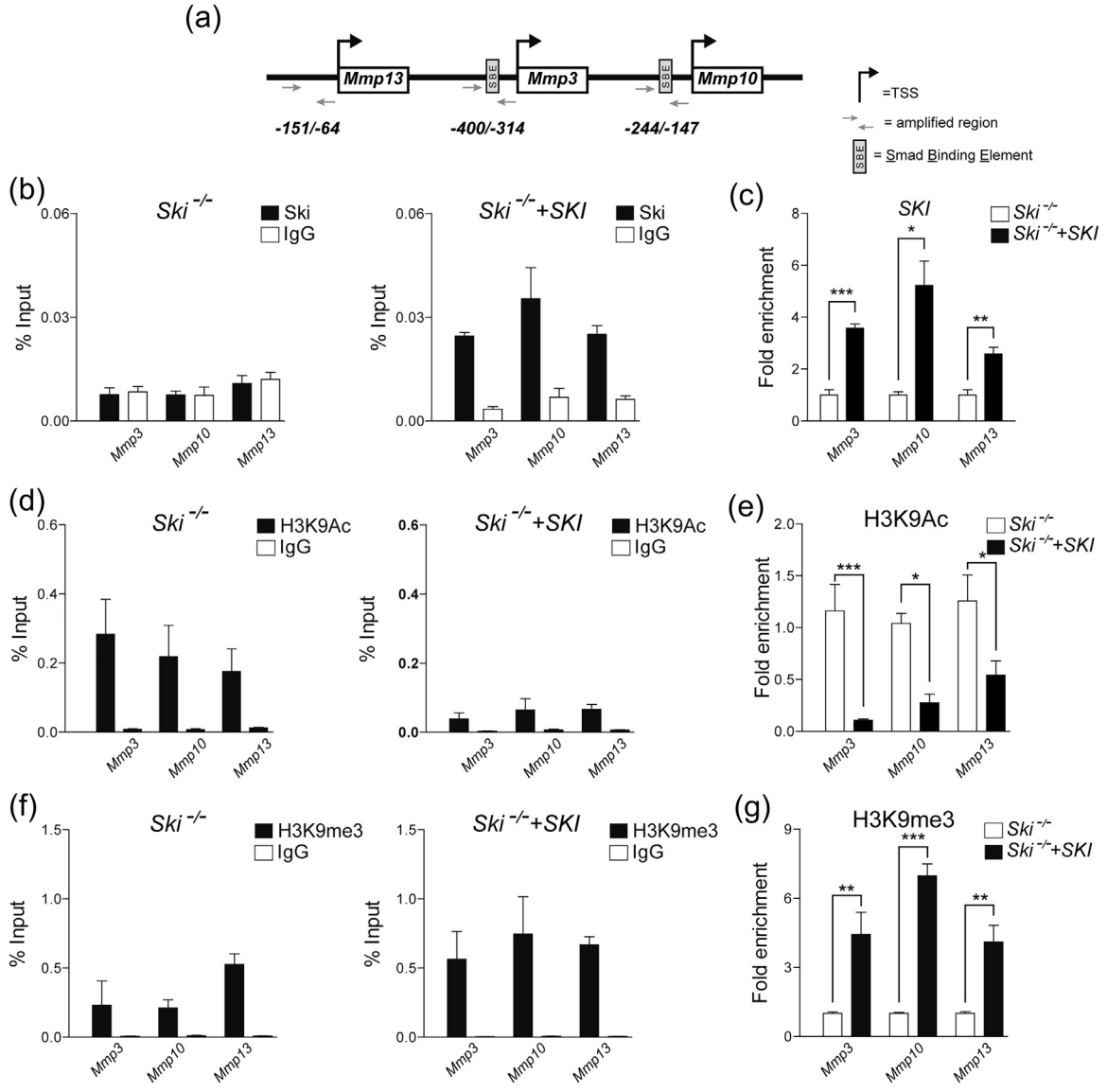

Figure 4. Ski occupies the promoter of *Mmp* 3, 10 and 13 genes, and its presence is associated with decreased H3K9ac and increased H3K9me3 levels in mitotic cells. Ski$^{-/-}$ + SKI and Ski$^{-/-}$ MEFs were cultured without Dox for 72 h and later synchronised in M phase. ChIP-qPCR experiments in mitotic MEFs were performed to validate Ski target genes. (a) Schematic representation of the position of the primers used to identify the localisation of Ski in the promoter of the three *Mmp* genes (grey arrows). The SBE Box indicates the position of SBEs. (b) Detection of Ski in the promoter of target *Mmp* genes in control Ski$^{-/-}$ (Left panel) and Ski$^{-/-}$ + SKI MEFs (right panel). (c) Enrichment of Ski in the promoter of *Mmp* genes. The promoter of *Gapdh* was used as an internal control. (d) Detection of H3K9ac mark in the promoter of *Mmp* genes in Ski$^{-/-}$ (left panel) and Ski$^{-/-}$ + SKI (right panel) MEFs. (e) Enrichment of H3K9ac calculated by comparing the percentage of input in Ski$^{-/-}$ and Ski$^{-/-}$ + SKI MEFs. (f) Detection of H3K9me3 in the promoter of *Mmp* genes in Ski$^{-/-}$ (Left panel) and Ski$^{-/-}$ + SKI MEFs (right panel). (g) Enrichment of H3K9me3 calculated by comparing the percentage of input in Ski$^{-/-}$ and Ski$^{-/-}$ + SKI MEFs. All experiments were performed at least three times, each time in triplicates. *$p < .05$, **$p < .01$ and ***$p \leq .001$; two-tailed *t*-test.

Consistent with the effect that the presence of Ski has on H3K9ac/me3 in MaSat regions, the levels of H3K9ac in *Mmp* 3, *Mmp* 10 and *Mmp* 13 promoters were higher in Ski$^{-/-}$ MEFs compared to Ski$^{-/-}$ + SKI cells (Figure 4(d) and (e)). By contrast, there is a higher enrichment of H3K9me3 at the promoters of the analysed genes in Ski-expressing cells (Figure 4(f) and (g)).

To evaluate whether the Ski-dependent repression of *Mmp* 3, *Mmp* 10 and *Mmp* 13 genes remains throughout the cell cycle, the association of Ski to the promoter of these genes was assessed in interphase nuclei. Ski occupies the promoter of *Mmp* genes during interphase (Figure 5(a)). Moreover, the absence of the protein was associated with lower H3K9me3 and higher H3K9ac levels (Figure 5(b)–(e)). Accordantly, the expression of *Mmp3* and *Mmp10* genes was repressed in Ski-expressing cells beyond the early G_1 phase of the cell cycle (Figure 5(f)).

Altogether, these results indicate that the presence of Ski at the promoters of *Mmp 3*, 10 and 13 genes in the mitotic chromosome 9 would regulate H3K9ac/me3 levels. In this way, the expression of these genes remains repressed once the cell cycle resumes. Considering the overall results, it is likely that the Ski-dependent repressive regulation of *Mmp* genes would also apply to other loci nearby the pericentromeric regions of chromosomes occupied by Ski during mitosis.

Ski$^{-/-}$ MEFs display an increased Mmp 3 activity and invasion capability

To evaluate whether the over-expression of *Mmp* 3 gene in Ski$^{-/-}$ MEFs results in increased catalytic activity, zymography was performed using casein as a substrate, which is efficiently degraded by the caseolytic activity of Mmp3 among other proteases, but not by Mmp 10 and Mmp 13 [57]. As expected, caseolytic activity is significantly higher in Ski$^{-/-}$ MEFs compared to Ski$^{-/-}$ + Ski or WT Ski$^{+/+}$ MEFs (Figure 6(a)). In the same way, invasiveness of WT, Ski$^{-/-}$ and Ski$^{-/-}$ + SKI MEFs was evaluated using a Matrigel assay to mimic the ECM. Ski$^{-/-}$ MEFs are approximately three times more invasive compared to WT or Ski$^{-/-}$ + SKI MEFs (Figure 6(b) and (c)).

Discussion

Ski is a transcriptional co-repressor that negatively regulates TGF-β signalling [31,36–38,53,58,59]. It is a nuclear protein, although it has also been described in the cytoplasm [60,61] and associated with mitotic spindles and centrosomes [48,49]. Herein, we describe for the first time that Ski remains associated with the chromosomes during mitosis in mouse fibroblasts, specifically in the pericentromeric region, where the protein is detected as a distinct dot on each sister chromatid and is associated with MaSat DNA (Figure 1). Due to the polyploidy of our model, we could not identify the exact number of chromosomes containing Ski. Nevertheless, results from diploid primary MEFs indicate that the number of chromosomes occupied by Ski in mitosis is variable, with mostly with four per metaphase (Supplementary Figure 1). In this work, we confirm the association of Ski with one of these chromosomes: chromosome 9. Differential gene expression in early G_1 cells suggests that Ski would also occupy chromosomes 13 and 14 during mitosis. However, further studies are required to confirm this hypothesis.

We found that the re-establishment of Ski expression induces loss of H3K9ac and increase levels of H3K9me3 in MaSat during mitosis (Figure 2). In this phase, HDACs are displaced from chromatin [62], so if there was a direct deacetylation mechanism guided by Ski and HDACs, this might occur before entry into mitosis, for instance, during DNA replication [63]. Nevertheless, HDACs have additional essential roles during mitosis. For instance, HDAC3 remains attached to the mitotic spindle and plays a role in microtubule and kinetochore attachment [64]. Besides, it is involved in modulating AurKB activity on H3S10 [65]. Moreover, the use of HDAC inhibitors induces chromosome instability [66], mitotic slippage [67], pericentromeric heterochromatin disruption [68,69], and alterations in the kinetochore assembly [69].

In early G_1 cells, Ski is associated with repression of genes that are located mostly on chromosome 13 and in regions of chromosome 9 that are close to pericentromeric heterochromatin (Chr.9A, Figure 3 and Table 1).

The most repressed genes in the presence of Ski are *Mmp3*, *Mmp10* and *Mmp13*. These genes are immersed in the pericentromeric heterochromatin, surrounded by MaSat in chromosome 9. According to these results, Ski$^{-/-}$ MEFs have higher Mmp3 activity and invasion capability than cells expressing Ski (Figure 6). These characteristics are associated with ECM remodelling and are consistent with the described role for Ski in kidney fibrosis [70,71], wound healing and scar formation [72]. These processes are dependent on TGF-β/Smad activation and collagen I production [73–75]. Consistently with Ski's repressor activity of the TGF-β pathway [39,40,53], KEEG analysis of microarray data for genes located in the first 50 Mb of chromosomes showed that TGF-β signalling was differentially expressed in MEFs lacking Ski.

The increased Ski-dependent H3K9me3 at the promoters of *Mmp* 3, 10 and 13 strongly suggests that the repression of these genes observed in early G_1 and throughout the cell cycle is dependent on the occupancy of these promoters by Ski in mitosis and interphase (Figures 4 and 5). This regulation might be lost upon the presence of physiological or

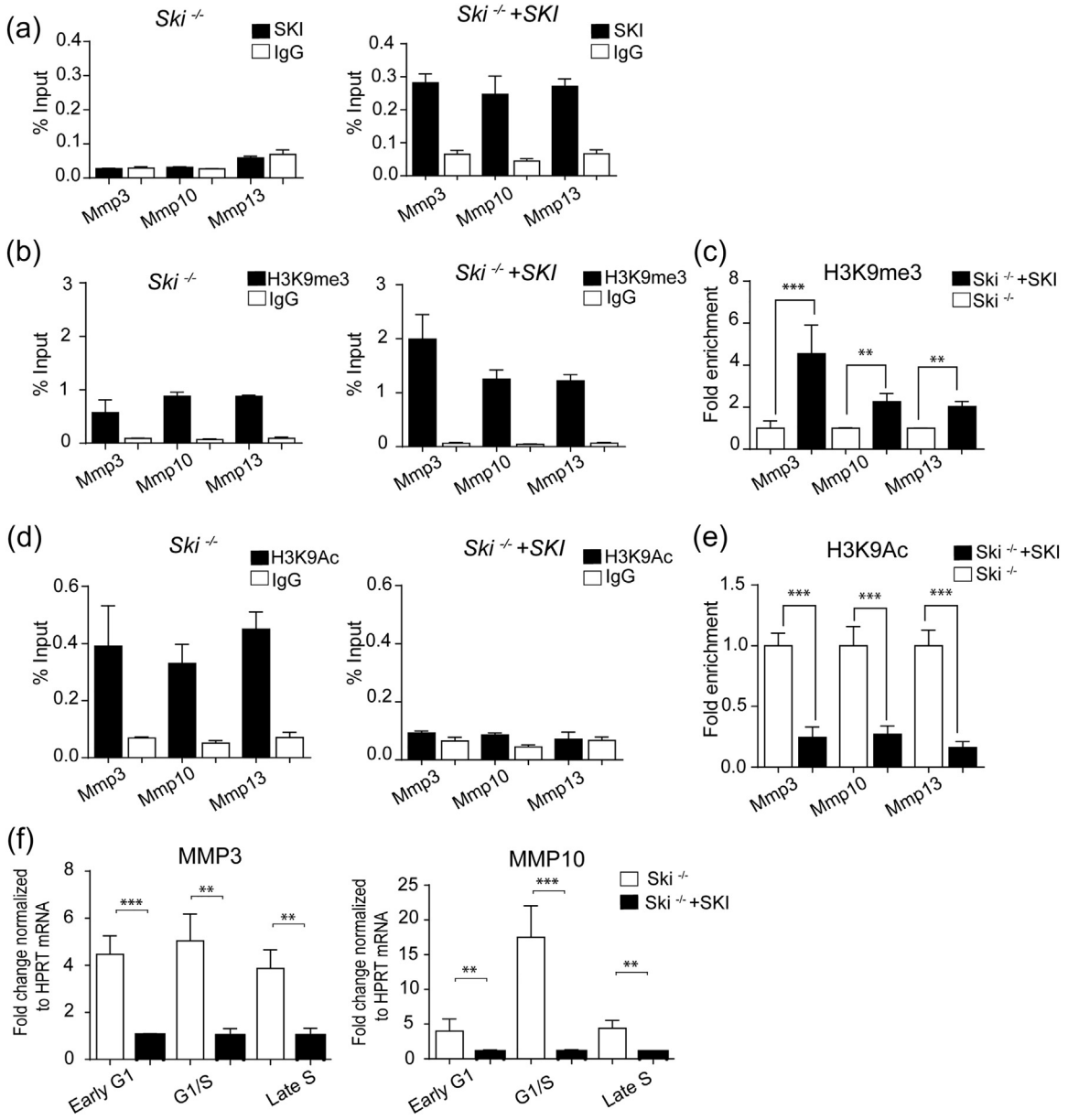

Figure 5. Ski occupies the promoter of *Mmp* 3, 10 and 13 genes, and its presence is associated with decreased H3K9ac, increased H3K9me3 levels and reduced expression of the genes during interphase. Ski$^{-/-}$ + SKI and Ski$^{-/-}$ MEFs were cultured without Dox for 72 h. ChIP-qPCR experiments were performed as in Figure 4. (a) Detection of Ski in the promoter of target *Mmp* genes in control Ski$^{-/-}$ (Left panel) and Ski$^{-/-}$ + SKI MEFs (right panel). (b) Detection of H3K9me3 mark in the promoter of *Mmp* genes in Ski$^{-/-}$ (left panel) and Ski$^{-/-}$ + SKI (right panel) MEFs. (c) Enrichment of H3K9me3 calculated by comparing the percentage of input in Ski$^{-/-}$ and Ski$^{-/-}$ + SKI MEFs. (d) Detection of H3K9ac in the promoter of *Mmp* genes in Ski$^{-/-}$ (left panel) and Ski$^{-/-}$ + SKI MEFs (right panel). (e) Enrichment of H3K9ac calculated by comparing the percentage of input in Ski$^{-/-}$ and Ski$^{-/-}$ + SKI MEFs. (f) mRNA expression levels of Mmp3 and Mmp10 in Ski$^{-/-}$ and Ski$^{-/-}$ + SKI MEFs synchronised at different stages of the cell cycle. Results are normalised to HPRT mRNA levels. All experiments were performed at least three times, each time in triplicates. $^{**}p < .01$ and $^{***}p \leq .001$; two-tailed *t*-test.

pathological signals. During early G_1, the expression of numerous genes located close to pericentromeric heterochromatin was also affected by the presence of Ski (Figure 3), suggesting that the effect of Ski on those genes may be direct, as it is for *Mmp3*, *Mmp10* and *Mmp13*. Nevertheless, it is also plausible to hypothesise that the presence of Ski in a particular region, i.e. SBE-containing promoters, would favour

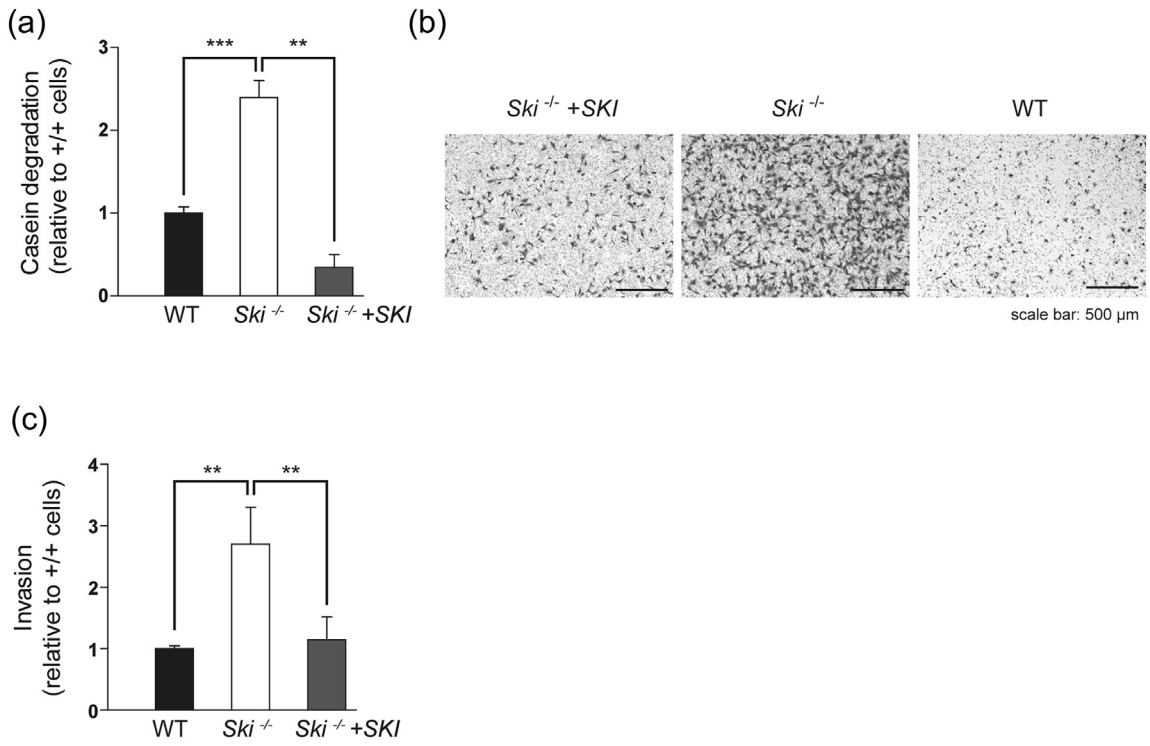

Figure 6. Ski knock out cells show enhanced proteolytic activity and invasion capability. (a) Conditioned medium of WT, $Ski^{-/-}$ and $Ski^{-/-}$ + SKI MEFs was collected and run in a non-denaturing SDS-PAGE, using casein as substrate. Results are expressed as fold change relative to WT MEFs. B and C) WT, $Ski^{-/-}$ and $Ski^{-/-}$ + SKI MEFs were plated into Matrigel pre-coated Transwell chambers. After 22 h, invasive cells were stained and counted in at least three light microscope fields. Results are expressed as fold change relative to WT MEFs. Data represent mean ± SE for three independent experiments. ** $p < .01$ and *** $p < .001$. Two-way ANOVA.

the establishment and spread of H3K9me3 to near chromosomal regions, affecting more distant loci. This has been described for Pax 3/9 transcription factors in mouse pericentromeric DNA [76] and in pluripotent stem cells [77]. On the other hand, for those genes located far from pericentromeric regions and affected by the absence of Ski, the effect may be indirect, through the regulation of transcription factors, both repressors and activators of transcription.

Although previous studies suggest that TGF-β signalling regulates mitotic progression, the role of the TGF-β pathway in mitosis is not well understood. For instance, in bone marrow stromal cells, TGF-β/Smad3 signalling is necessary to regulate the APC-Separase complex during chromosome segregation [78]. Ski has also been associated with the negative regulation of TGF-β signalling during mitosis. Ski localises to the mitotic spindle [48,49] where it interacts with Smad3, inhibiting Smad2/3 complex activation in the absence of TGF-β. Zieba *et al.* described the association of Ski with chromatin through the Smad proteins during mitosis [79]. Although these authors did not visualise Ski on chromosomes, by using an *in vivo* proximity ligation assay, they showed that Ski forms complexes with phosphorylated Smad2/3 and is located at mitotic chromatin in naturally transformed human keratinocyte like cells treated with a TGFβ-RI inhibitor [79]. Whether the effects of Ski reported in their work were due to repression of TGF-β signalling remains an open question.

During mitosis, several transcription factors involved in regulating cell fate bind to mitotic chromosomes, regulating the expression of lineage-specific genes. For example, Gata1 and FoxA1, required for haematopoiesis and liver differentiation, respectively; and Esrrb, Oct4, Klf4 and Sox2, transcription factors that sustain pluripotency and promote mouse ESC self-renewal [13,14,26,77]. Although this mechanism, known as mitotic bookmarking, has been described as a central epigenetic mechanism to maintain cellular identity through cell divisions, emerging evidence indicates that mitotic bookmarking might also contribute to coordinate cell proliferation and growth [80].

Thus, although our results do not permit to conclude that Ski is a mitotic bookmarking factor, the repression mediated by this protein may be important to maintain cell identity after cell division or also to regulate highly controlled processes such as the G_1-S transition.

On the other hand, hypomethylation of pericentromeric DNA has been reported in tumours [81–84]. H3K9me3 in MaSat is recognised by the heterochromatin protein HP1 [85,86]. In addition to H3K9me3, HP1 binds to a variety of interaction partners such as histone methyltransferases, DNA methyltransferases, Methyl-CpG binding protein MeCP2 and others. Thus, HP1 serves as a platform for the recruitment of downstream factors and heterochromatin formation [21,87–90]. Accordingly, hypomethylation of pericentromeric regions results in chromosomal missegregation, chromosomal rearrangements, reduced centromere condensation, micronuclei formation and tumourigenesis [91,92]. Ski$^{-/-}$ MEFs exhibit lagging chromosomes, chromatin/chromosome bridges, micronuclei and aneuploidy [52]. Thus, loss of H3K9me3 in Ski$^{-/-}$ MEFs could at least partially explain the chromosomal segregation defects and aneuploidy observed in these cells.

Whereas pericentromeric heterochromatin provides a structural scaffold for centromere formation and is essential for the safeguard of chromosome stability [20,23,68,91,93,94], the effect that hypomethylation of these regions might have on the expression of nearby genes has not been extensively studied so far.

Here, we propose a model where Ski remains associated with specific chromosomes at pericentromeric DNA in mitosis, driving methylation of H3K9 at MaSat and promoters of neighbouring genes, hence controlling chromosome heterochromatin structure, while preserving the repressive marks in genes which must be kept silenced once the transcriptional program is resumed after cell division.

Methods

Cell culture, transfection and cell cycle synchronisation

Ski$^{-/-}$ MEFs were kindly provided by Dr. Colmenares [95]. Ski$^{-/-}$ MEFs expressing the human Ski cDNA under control of a TET-OFF regulated promoter (Ski$^{-/-}$ + SKI MEF) were described before [52]. Ski$^{-/-}$ + SKI MEFs were kept in doxycycline (2 μg/ml) and released for 72 h in fresh medium to perform the experiments. MEFs and NIH-3 T3 cells were cultured in “Dulbecco's modified Eagle medium” (DMEM) supplemented with 10% of foetal bovine serum (Gibco, 12483020) or 10% of calf serum (Merck, C8056), respectively, and were maintained at 37 °C and 5% of CO_2.

Ski$^{-/-}$ + SKI MEF and NIH3T3 cells were transfected with a REBNA-GFP-Ski vector, and the selection was performed as described before [52]. GFP-Ski construct was obtained by cloning hSki cDNA into the pEGFP-C1 vector (Clontech, Cat. 6084-1). MEFs and NIH-3 T3 were synchronised in M and early G_1 phases of the cell cycle. Cells were firstly synchronised in S phase by double thymidine block, using 120 mM of thymidine (Sigma-Aldrich, T9250) for 16 h; then, cells were released in serum-free medium for 10 h, followed by a second block (120 mM thymidine for 16 h). After the second block, the cells were rinsed and released in media containing 300 μg/ml of Colcemid (Sigma-Aldrich, 10295892001). Mitotic cells were collected by mitotic shake-off. To obtain cells in early G_1, mitotic cells were cultured in fresh media for 2 h, when most cells were attached and finishing cytokinesis. Cell cycle synchronisation was monitored by flow cytometry using propidium iodide (Sigma-Aldrich, P4170) as a DNA label.

Indirect immunofluorescence

For conventional IIF, Ski$^{-/-}$ + SKI, Ski$^{-/-}$ MEF and NIH-3 T3 were cultured in 110-mm cover glass, fixed in 3.7% paraformaldehyde solution (Sigma-Aldrich, 252549) for 10 min at room temperature (RT) and permeabilized with 0.25% Triton X-100/phosphate-buffered saline at RT, followed by blocking in 3% bovine serum albumin (BSA). Primary antibodies used were as follows: human anti-Crest (Antibodies Incorporated 1:300), rabbit anti-Ski (H-329 Santa Cruz Biotechnologies, sc-9140 1:200), mouse anti-Ski (G8, Millipore, MABE442 1:50), rabbit anti-H3K9ac (Abcam, ab12179 1:1000) and anti-GFP Atto488 (GFP-Booster 1:100). Secondary antibodies used were as follows: goat anti-rabbit IgG (H + L) Alexa Fluor 488 (Molecular Probes, Invitrogen™, A-11008), goat anti-rabbit IgG (H + L) Alexa Fluor 594 (Molecular Probes, Invitrogen™, A-11037) and goat anti-mouse IgG (H + L) Alexa Fluor 594 (Molecular Probes, Invitrogen™, A-11032); all secondary antibodies were diluted 1:500 in 1% BSA/0.05% Triton X100. Nuclei were stained with 0.05 μg/ml DAPI (Molecular Probes, Invitrogen™, D1306) for 5 min at 4 °C.

Metaphase chromosome spreads and IIF

NIH-3 T3, Ski$^{-/-}$ + SKI MEF and Ski$^{-/-}$ MEF were synchronised in M phase and separated by mitotic shake-off. Mitotic cells were swollen in hypotonic solution (75 mM KCl) for 15 min at 37 °C, and adhered to the positively charged microscope slides (Cellpath MDB-0102-54A) by cytocentrifugation for 15 min at 1500 rpm. Then, the slides were incubated with potassium chromosomes media (120 mM KCl/20 mM NaCl/10 mM Tris–HCl (pH 7.5)/0.5 mM EDTA/0.1% Triton X-100) for 5 min at RT to eliminate the cellular membranes and stabilise the chromosomes [96]. The fresh metaphase spreads were incubated with primary and secondary antibodies diluted in 1% BSA/0.5%, TritonX100/potassium chromosomes media, fixed with 3.7% of paraformaldehyde

solution, and finally stained with 0.05 DAPI µg/ml. Fixation protocol was optimised to obtain a clear image of Ski's signal on chromosomes (Supplementary Figure 4A).

Differential gene expression at early G_1 phase

$Ski^{-/-}$ and $Ski^{-/-}$ + SKI MEF were synchronised at early G_1 phase, and total RNA was extracted using Qiagen RNAeasy kit (Qiagen, Valencia, CA). RNA was quantified by OD 260/280 nm (accepted ratio <1.9) and 18S/28S ratio was semi-quantified (accepted ratio <1.6). A total amount of 12 µg of RNA was used to synthesise cDNA fluorescent probes in the presence of Cy3 or Cy5 conjugated UTP nucleotides. The efficiency of fluorescent dye incorporation was evaluated at 550 nm.

An equimolar mix of each cDNA obtained from $Ski^{-/-}$ and $Ski^{-/-}$ + SKI MEFs were hybridised on MEEBO microarray slides. The hybridisation was performed in 25% deionised formamide (Sigma Aldrich, F9037), 0.005% SDS and 5 µg of DNA from salmon sperm (Invitrogen, 15632011). The experiment was performed using the dye swap approach to avoid interferences associated with the inherent fluorescence of Cy3 and Cy5 molecules. The mixture was denatured at 90 °C for 5 min and incubated on the chip for 20 h at 42 °C. Then, the microarray chip was washed, dried and scanned in a ScanArray Lite (PerkinElmer Life Sci. Inc., Waltham, MA).

The resulted TIFF files were analysed using GenePix Pro 6.0 software, and data were deposited in the microarray database NCI (mAdb, http://nciarray.nci.nih.gov). The annotated data were downloaded from mAdb for normalisation using the "print-tip loss" in the DNMAD platform (http://dnmad.bioinfo.cnio.es/) [97]. Normalised data were filtered and inputted (67% in KNN) in *the pre*P platform (http://prep.bioinfo.cnio.es/) [98].

The hybridised probes that passed all data filtering were used to assess differential gene expression using the Significance Analysis of Microarrays algorithm in TmeV software [99]; a *q*-value of 0.149 was automatically calculated for false discovery rate estimation.

The genes that were selected in this work for further studies were validated by qPCR using specific primers listed in the supplementary material (Table S1).

Chromatin immunoprecipitation

$Ski^{-/-}$ and $Ski^{-/-}$ + SKI MEFs synchronised in M phase or in interphase were used in a ChIP protocol. Cells were fixed using 3.7% paraformaldehyde (Sigma-Aldrich, 252549) in phosphate-buffered saline at RT for 10 min and quenched with glycine to a final concentration of 0.125 M for 5 min at RT. Fixed cells were lysed in lysis buffer (50 mM Hepes (pH 7.8), 3 mM $MgCl_2$, 20 mM KCl, 0.1% NP-40, and proteinase inhibitors cocktail immediately before use). Chromatin shearing was performed in sonication buffer (50 mM Hepes (pH 7.9), 140 mM NaCl, 1 mM EDTA, 1% Triton X-100, 0.1% deoxycholate acid, 0.1% SDS, and proteinase inhibitors cocktail immediately before use), using a Bioruptor bath sonicator (Diagenode, NJ, USA) with 3 cycles of 10 min (Power level: Medium, Lapse 30seg On/Off). Chromatin of 25 µg was used for immunoprecipitation. Samples were re-suspended in sonication buffer to a final volume of 450 µl and then pre-cleared with 4 µg of normal IgG and 40 µl of protein A or G-coated agarose beads (Santa Cruz Biotechnology, sc-2001, sc-2002) for 2 h at 4 °C. After pre-clearing, samples were washed and the beads were discarded. The cleared supernatant was incubated overnight at 4 °C with 4 µg of specific antibody. The antibodies used are rabbit anti-H3 (Abcam, ab1791), rabbit anti-H3K9ac (Abcam, ab12179), rabbit anti-H3K9me3 (Abcam, ab8898) and rabbit anti-Ski (H-329, Santa Cruz Biotechnologies, sc-9140). Non-specific rabbit IgG (Santa Cruz Biotechnologies, sc-2027) was used as a control antibody for ChIP.

After incubation, the antibody–antigen complexes were captured with 40 µl of protein A or G-coated agarose beads in a rotator for 2 h at 4 °C. After the incubation, the beads were pelleted and separated from the supernatant to proceed with the washing steps: once with sonication buffer, two times with immunoprecipitation wash buffer (100 mM Tris–HCl (pH 8.0), 500 mM LiCl, 1% NP-40, and 1% deoxycholic acid), and once in TE buffer (pH 8.0). DNA was eluted in 100 µl of elution buffer (50 mM $NaHCO_3$ and 1% SDS) and incubated for 15 min at 65 °C. After elution, the chromatin was resuspended and de-crosslinked in sonication buffer with 2 µg of RNase A overnight at 65 °C and treated with 50 µg of proteinase K (Sigma Aldrich, P2308) 2 h at 50 °C. De-crosslinked chromatin was then purified using phenol–chloroform extraction and finally evaluated by qPCR using specific primers (Table S1). As a positive control for Ski antibody, the Smad7 promoter [53] was immunoprecipitated in non-synchronised WT MEFs (Supplementary Figure 4B).

Invasion assay on Matrigel layer

Cell invasion was measured via the transwell chamber invasion assay. Briefly, cells (2.5×10^4 cells/well) were seeded into the top of the upper chamber (8-µm-pore Boyden chambers coated with Matrigel, Becton Dickinson-BioCoat™ Matrigel™) in 500 µl of serum-free DMEM. The wells were filled with 5% FBS DMEM as a chemoattractant (conditioned medium). Then the cells were allowed to invade toward conditioned medium for 22 h. Finally, cells adhered to the upper surface of the filter were removed using a cotton applicator. The invading

cells were stained with 0.1% crystal violet solution in 20% methanol, photographed using the Cytation3 equipment (Biotek Inc) and counted. The data represent three independent experiments.

Caseinolytic zymography assay

Cells were cultured for 48 h to obtain 90% confluence. The growth medium was changed to serum-free DMEM, and cells were kept for 30–36 h. The medium was collected and centrifuged at 1500***g*** for 10 min at 4 °C. Supernatant was mixed with loading buffer, under non-reducing conditions (10% v/v glycerol, 2% SDS, 62.5 mM Tris (pH 6.8), 0.02% bromophenol blue), and run in a 10% Tris/HCl acrylamide gel containing 0.1% casein. Electrophoresis was performed at 120 V at 4 °C for approximately 2–2.5 h. Resolved proteins were renatured by incubation of the gels in 2.5% Triton X-100 solution for 30 min at RT. Next, gels were quickly washed three times in water, and then incubated in zymography buffer (50 mM Tris/HCl (pH 8.0), 200 mM NaCl, 1.25 mM $CaCl_2$) overnight at 37 °C. Caseinolytic activity in the gels was visualised as negative staining with Coomassie brilliant blue.

Statistical analysis

The Student *t*-test was used to compare qPCR and ChIP-qPCR results. The two-way ANOVA test was used in the Invasion and Caseolityc assay. A p-value <0.05 was considered as significant.

Acknowledgments

This work was financially supported by the National Commission for Scientific and Technological Research (CONICYT), Chile, through the following Programs: FONDECYT 1151435 and 1120222; PIA ACT172101; FONDAP 15090007; and Chilean doctoral fellowship 21110559.

Author Contributions

C.C., H.S., U.U., R.A., M.M. and K.M. conceived and designed the experiments. C.C., H.S., V.P., S. R., G.D., D.C., M.G., M.a.M., E.C., A.S. and E.S. performed experiments. C.C., S.R. and K.M. wrote, reviewed and edited the manuscript. All authors revised and approved the manuscript.

Additional Information

The authors declare no competing interests.

Appendix A. Supplementary data

Supplementary data to this article can be found online at https://doi.org/10.1016/j.jmb.2020.03.013.

Received 24 October 2019;
Received in revised form 23 February 2020;
Accepted 11 March 2020
Available online 19 March 2020

Keywords:
Ski;
MMP;
mitotic bookmarking;
H3K9me3;
MaSat

Abbreviations used:
MEF, mouse embryonic fibroblast; MaSat, major satellite; ChIP, chromatin immunoprecipitation; HDAC, histone deacetylases; WT, wild-type; MiSat, minor satellite; MEEBO, Mouse Exonic Evidence-Based Oligonucleotide; SBE, Smad binding element; ECM, extracellular matrix; DMEM, Dulbecco's modified Eagle medium; IIF, indirect immunofluorescence; RT, room temperature; BSA, bovine serum albumin.

References

[1] Y. Ma, K. Kanakousaki, L. Buttitta, How the cell cycle impacts chromatin architecture and influences cell fate, Front. Gen. 5 (2015) 1–18, https://doi.org/10.3389/fgene.2015.00019FEB.
[2] M. a Martínez-Balbás, a Dey, S.K. Rabindran, K. Ozato, C. Wu, Displacement of sequence-specific transcription factors from mitotic chromatin, Cell 83 (1) (1995) 29–38, https://doi.org/10.1016/0092-8674(95)90231-7.
[3] K.V. Prasanth, P.A. Sacco-Bubulya, S.G. Prasanth, D.L. Spector, Sequential entry of components of the gene expression machinery into daughter nuclei, Mol. Biol.Cell 14 (3) (2003) 1043–1057, https://doi.org/10.1091/mbc.E02-10-0669.
[4] G.G. Parsons, C.A. Spencer, Mitotic repression of RNA polymerase II transcription is accompanied by release of transcription elongation complexes, Mol. Cell. Biol. 17 (10) (1997) 5791–5802, https://doi.org/10.1128/MCB.17.10.5791.
[5] J.M. Gottesfeld, D.J. Forbes, Mitotic repression of the transcriptional machinery, Trends Biochem. Sci. 22 (6) (1997) 197–202, https://doi.org/10.1016/S0968-0004(97)01045-1.
[6] K.C. Palozola, H. Liu, D. Nicetto, K.S. Zaret, Low-level, global transcription during mitosis and dynamic gene reactivation during mitotic exit, Cold Spring Harb. Symp. Quant. Biol. 34280 (2018) https://doi.org/10.1101/sqb.2017.82.034280LXXXII.
[7] K.C. Palozola, G. Donahue, H. Liu, G.R. Grant, J.S. Becker, A. Cote, H. Yu, A. Raj, et al., Mitotic transcription and waves of gene reactivation during mitotic exit, Science 6359 (2017) 119–122.
[8] I.J. de Castro, E. Gokhan, P. Vagnarelli, Resetting a functional G1 nucleus after mitosis, Chromosoma. 125 (2016) 607–619, https://doi.org/10.1007/s00412-015-0561-6.
[9] R. Duncan, L. Bazar, G. Michelotti, T. Tomonaga, H. Krutzsch, M. Avigan, D. Levens, A sequence-specific, single-strand

binding protein activates the far upstream element of c-myc and defines a new DNA-binding motif, Genes Dev. 8 (4) (1994) 465–480, https://doi.org/10.1101/gad.8.4.465.
[10] G.A. Michelotti, E.F. Michelotti, A. Pullner, R.C. Duncan, D. Eick, D. Levens, Multiple single-stranded cis elements are associated with activated chromatin of the human c-myc gene in vivo, Mol. Cell. Biol. 16 (6) (1996) 2656–2669.
[11] D.W. Young, M.Q. Hassan, X. Yang, M. Galindo, A. Javed, S. K. Zaidi, G.S. Stein, Mitotic retention of gene expression patterns by the cell fate-determining transcription factor Runx2, Proc. Natl. Acad. Sci. U. S. A. (104) (2007) 3189–3194, https://doi.org/10.1073/pnas.0611419104.
[12] S. Kadauke, M.I. Udugama, J.M. Pawlicki, J.C. Achtman, D. P. Jain, Y. Cheng, R. Hardison, G.a. Blobel, Tissue-specific mitotic bookmarking by hematopoietic transcription factor GATA1, Cell 150 (4) (2012) 725–737, https://doi.org/10.1016/j.cell.2012.06.038.
[13] J.M. Caravaca, G. Donahue, J.S. Becker, X. He, C. Vinson, K.S. Zaret, Bookmarking by specific and nonspecific binding of FoxA1 pioneer factor to mitotic chromosomes, Genes Dev. 27 (2013) 251–260, https://doi.org/10.1101/gad.206458.112.
[14] N. Festuccia, A. Dubois, S. Vandormael-Pournin, E. Gallego Tejeda, A. Mouren, S. Bessonnard, F. Mueller, C. Proux, et al., Mitotic binding of Esrrb marks key regulatory regions of the pluripotency network, Nat. Cell Biol. 18 (11) (2016) 1139–1148, https://doi.org/10.1038/ncb3418.
[15] M.E. Oomen, A. Hansen, Y. Liu, X. Darzacq, J. Dekker, CTCF sites display cell cycle dependent dynamics in factor binding and nucleosome positioning, BioRxiv. 29 (2018) 236–249, https://doi.org/10.1101/365866.
[16] S.S. Teves, L. An, A. Bhargava-Shah, L. Xie, X. Darzacq, R. Tjian, A stable mode of bookmarking by TBP recruits RNA polymerase II to mitotic chromosomes, ELife. Vol. 7 (2018) https://doi.org/10.7554/eLife.35621.
[17] T. Hashimshony, J. Zhang, I. Keshet, M. Bustin, H. Cedar, The role of DNA methylation in setting up chromatin structure during development, Nat. Genet. 34 (2003) 187–192, https://doi.org/10.1038/ng1158.
[18] H. Hashimoto, P.M. Vertino, X. Cheng, Molecular coupling of DNA methylation and histone methylation, Epigenomics 2 (5) (2010) 657–669, https://doi.org/10.2217/epi.10.44.
[19] P. Jeppesen, A. Mitchell, B. Turner, P. Perry, Antibodies to defined histone epitopes reveal variations in chromatin conformation and underacetylation of centric heterochromatin in human metaphase chromosomes, Chromosoma. 5–6 (1992) 322–332, https://doi.org/10.1007/BF00346011.
[20] M. Guenatri, D. Bailly, C. Maison, G. Almouzni, Mouse centric and pericentric satellite repeats form distinct functional heterochromatin, J. Cell Biol. 166 (4) (2004) 493–505, https://doi.org/10.1083/jcb.200403109.
[21] W. Fischle, B.S. Tseng, H.L. Dormann, B.M. Ueberheide, B.A. Garcia, J. Shabanowitz, C.D. Allis, Regulation of HP1-chromatin binding by histone H3 methylation and phosphorylation, Nature 438 (7071) (2005) 1116–1122, https://doi.org/10.1038/nature04219.
[22] R.K. Ng, J.B. Gurdon, Epigenetic memory of an active gene state depends on histone H3.3 incorporation into chromatin in the absence of transcription, Nat. Cell Biol. 10 (1) (2008) 102–109, https://doi.org/10.1038/ncb1674.
[23] A.H.F.M. Peters, O. Carroll, H. Scherthan, K. Mechtler, S. Sauer, C. Schöfer, K. Weipoltshammer, M. Pagani, et al., Loss of the Suv39h histone methyltransferases impairs mammalian heterochromatin and genome stability, Cell 107 (2001) 323–337.
[24] S.J. Nowak, V.G. Corces, Phosphorylation of histone H3: A balancing act between chromosome condensation and transcriptional activation, Trends Genet. 20 (2004) 214–220, https://doi.org/10.1016/j.tig.2004.02.007.
[25] D. Bonenfant, H. Towbin, M. Coulot, P. Schindler, D.R. Mueller, J. van Oostrum, Analysis of dynamic changes in post-translational modifications of human histones during cell cycle by mass spectrometry, Mol. Cell. Proteomics 6 (11) (2007) 1917–1932, https://doi.org/10.1074/mcp.M700070-MCP200.
[26] N. Festuccia, I. Gonzalez, N. Owens, P. Navarro, Mitotic bookmarking in development and stem cells, Development 20 (2017) 3633–3645, https://doi.org/10.1242/dev.146522.
[27] D.W. Young, M.Q. Hassan, J. Pratap, M. Galindo, S.K. Zaidi, S. Lee, X. Yang, R. Xie, et al., Mitotic occupancy and lineage-specific transcriptional control of rRNA genes by Runx2, Nature 445 (7126) (2007) 442–446, https://doi.org/10.1038/nature05473.
[28] N. Nomura, S. Sasamoto, S. Ishii, T. Date, M. Matsui, R. Ishizaki, Isolation of human cDNA clones of ski and the ski-related gene, sno, Nucl. Ac. Res. 17 (14) (1989) 5489–5500, https://doi.org/10.1093/nar/17.14.5489.
[29] P. Sutrave, T.D. Copeland, S.D. Showalter, S.H. Hughes, Characterization of chicken c-ski oncogene products expressed by retrovirus vectors, Mol. Cell. Biol. 10 (6) (1990) 3137–3144.
[30] T. Nagase, G. Mizugachi, Requirement of protein co-factor for the DNA-binding function of the human ski proto-oncogene product, Nucl. Ac. Res. 18 (2) (1990) 337–343.
[31] A. Tecalco-Cruz, D. Ríos-López, G. Vázquez-Victorio, R. Rosales-Alvarez, M. Macías-Silva, Transcriptional cofactors Ski and SnoN are major regulators of the TGF-β/Smad signaling pathway in health and disease, Nucl. Ac. Res. 46 (2018) 3412–3428, https://doi.org/10.1101/gr.230300.117.
[32] R. Nicol, E. Stavnezer, Transcriptional repression by v-Ski and c-Ski mediated by a specific DNA binding site, J. Biol. Chem. 273 (6) (1998) 3588–3597.
[33] T. Nomura, M. Khan, S. Kaul, H. Dong, R. Wadhwa, C. Colmenares, I. Kohno, S. Ishii, Ski is a component of the histone deacetylase complex required for transcriptional repression by Mad and thyroid hormone receptor, Genes Dev. 13 (1999) 412–423, https://doi.org/10.1101/gad.13.4.412.
[34] F. Tokitou, T. Nomura, M.M. Khan, S.C. Kaul, R. Wadhwa, T. Yasukawa, S. Ishii, Viral ski inhibits retinoblastoma protein (Rb)-mediated transcriptional repression in a dominant negative fashion, J. Biol. Chem. 274 (8) (1999) 4485–4488, https://doi.org/10.1074/jbc.274.8.4485.
[35] K. Luo, S.L. Stroschein, W. Wang, D. Chen, E. Martens, S. Zhou, Q. Zhou, The ski oncoprotein interacts with the Smad proteins to repress TGF-β signaling, Genes Dev. 13 (17) (1999) 2196–2206.
[36] S. Akiyoshi, H. Inoue, J. Hanai, K. Kusanagi, N. Nemoto, K. Miyazono, M. Kawabata, C-ski acts as a transcriptional co-repressor in transforming growth factor-β signaling through interaction with Smads, J. Biol. Chem. 274 (49) (1999) 35269–35277, https://doi.org/10.1074/jbc.274.49.35269.
[37] W. Xu, K. Angelis, D. Danielpour, M.M. Haddad, O. Bischof, J. Campisi, E.E. Medrano, Ski acts as a co-repressor with Smad2 and Smad3 to regulate the response to type beta transforming growth factor, Proc. Natl. Acad. Sci. U. S. A. 97 (11) (2000) 5924–5929, https://doi.org/10.1073/pnas.090097797.
[38] W. Chen, S.S. Lam, H. Srinath, C. a Schiffer, W.E. Royer, K. Lin, Competition between Ski and CREB-binding protein for

binding to Smad proteins in transforming growth factor-beta signaling, J. Biol. Chem. 282 (15) (2007) 11365–11376, https://doi.org/10.1074/jbc.M700186200.
[39] J. Wu, A.R. Krawitz, J. Chai, W. Li, F. Zhang, K. Luo, Y. Shi, Structural mechanism of Smad4 recognition by the nuclear oncoprotein Ski: insights on Ski-mediated repression of TGF-β, Signaling 111 (2002) 357–367.
[40] N. Ueki, M.J. Hayman, Direct interaction of Ski with either Smad3 or Smad4 is necessary and sufficient for Ski-mediated repression of transforming growth factor-beta signaling, J. Biol. Chem. 278 (35) (2003) 32489–32492.
[41] N. Ferrand, A. Atfi, C. Prunier, The oncoprotein c-Ski functions as a direct antagonist of the transforming growth factor-β type I receptor, Cancer Res. 70 (21) (2010) 8457–8466, https://doi.org/10.1158/0008-5472.CAN-09-4088.
[42] K. Kokura, S.C. Kaul, R. Wadhwa, T. Nomura, M.M. Khan, T. Shinagawa, S. Ishii, The Ski protein family is required for MeCP2-mediated transcriptional repression, J. Biol. Chem. 276 (36) (2001) 34115–34121, https://doi.org/10.1074/jbc.M105747200.
[43] P. Dai, T. Shinagawa, T. Nomura, J. Harada, S.C. Kaul, R. Wadhwa, S. Ishii, Ski is involved in transcriptional regulation by the repressor and full-length forms of Gli3, Genes Dev. 16 (22) (2002) 2843–2848, https://doi.org/10.1101/gad.1017302.
[44] N. Ueki, L. Zhang, M.J. Hayman, Ski negatively regulates erythroid differentiation through its interaction with GATA1, Mol. Cell. Biol. 24 (23) (2004) 10118–10125.
[45] M. Ritter, D. Kattmann, S. Teichler, O. Hartmann, M.K.R. Samuelsson, A. Burchert, A. Neubauer, Inhibition of retinoic acid receptor signaling by Ski in acute myeloid leukemia, Leukemia 20 (3) (2006) 437–443, https://doi.org/10.1038/sj.leu.2404093.
[46] H.L. Zhao, N. Ueki, K. Marcelain, M.J. Hayman, The Ski protein can inhibit ligand induced RARα and HDAC3 degradation in the retinoic acid signaling pathway, Biochem. Biophys. Res. Commun. 383 (1) (2009) 119–124, https://doi.org/10.1016/j.bbrc.2009.03.141.
[47] C. Feld, P. Sahu, M. Frech, F. Finkernagel, A. Nist, T. Stiewe, A. Neubauer, Combined cistrome and transcriptome analysis of SKI in AML cells identifies SKI as a co-repressor for RUNX1, Nucl. Ac. Res. 46 (7) (2018) 3412–3428, https://doi.org/10.1093/nar/gky119.
[48] K. Marcelain, M.J. Hayman, The Ski oncoprotein is upregulated and localized at the centrosomes and mitotic spindle during mitosis, Oncogene 24 (27) (2005) 4321–4329, https://doi.org/10.1038/sj.onc.1208631.
[49] Y. Chen, L. Pirisi, K.E. Creek, Ski protein levels increase during in vitro progression of HPV16-immortalized human keratinocytes and in cervical cancer, Virology. 444 (1–2) (2013) 100–108, https://doi.org/10.1016/j.virol.2013.05.039.
[50] M. Macdonald, Y. Wan, W. Wang, E. Roberts, T.H. Cheung, R. Erickson, X. Liu, Control of cell cycle-dependent degradation of c-Ski proto-oncoprotein by Cdc34, Oncogene 23 (33) (2004) 5643–5653, https://doi.org/10.1038/sj.onc.1207733.
[51] J. Mosquera, R. Armisen, H. Zhao, D.a. Rojas, E. Maldonado, J. Tapia, A. Colombo, M. Hayman, et al., Identification of Ski as a target for Aurora A kinase, Bioch. Bioph. Res. Com. 409 (3) (2011) 539–543, https://doi.org/10.1016/j.bbrc.2011.05.040.
[52] K. Marcelain, R. Armisen, A. Aguirre, N. Ueki, J. Toro, C. Colmenares, M.J. Hayman, Chromosomal instability in mouse embryonic fibroblasts null for the transcriptional co-repressor Ski, J. Cell. Physiol. 227 (1) (2012) 278–287, https://doi.org/10.1002/jcp.22733.
[53] T. Tabata, K. Kokura, P. Ten Dijke, S. Ishii, Ski co-repressor complexes maintain the basal repressed state of the TGF-beta target gene, SMAD7, via HDAC3 and PRMT5, Genes Cells 14 (1) (2009) 17–28, https://doi.org/10.1111/j.1365-2443.2008.01246.x.
[54] M. Ashburner, C. Ball, J. Blake, D. Botstein, Gene ontology: tool for the unification of biology, Nature 25 (1) (2000) 25–29, https://doi.org/10.1038/75556.Gene.
[55] K.Y. Oróstica, R.A. Verdugo, ChromPlot: visualization of genomic data in chromosomal context, Bioinformatics 32 (15) (2016) 2366–2368, https://doi.org/10.1093/bioinformatics/btw137.
[56] J. Wang, D. Duncan, Z. Shi, B. Zhang, WEB-based GEne SeT AnaLysis Toolkit (WebGestalt): update 2013, Nucl. Ac. Res. 41 (Web Server issue) (2013) W77, 83 https://doi.org/10.1093/nar/gkt439.
[57] G. Pintucci, P.J. Yu, R. Sharony, F.G. Baumann, F. Saponara, A. Frasca, P. Mignatti, Induction of stromelysin-1 (MMP-3) by fibroblast growth factor-2 (FGF-2) in FGF-2 –/– microvascular endothelial cells requires prolonged activation of extracellular signal-regulated kinases-1 and -2 (ERK-1/2), J. Cell. Biochem. 90 (5) (2003) 1015–1025, https://doi.org/10.1002/jcb.10721.
[58] C. Jacob, H. Grabner, S. Atanasoski, U. Suter, Expression and localization of Ski determine cell type-specific TGFbeta signaling effects on the cell cycle, J. Cell Biol. 182 (3) (2008) 519–530, https://doi.org/10.1083/jcb.200710161.
[59] J. Deheuninck, K. Luo, Ski and SnoN, potent negative regulators of TGF-beta signaling, Cell Res. 19 (1) (2009) 47–57, https://doi.org/10.1038/cr.2008.324.
[60] E.E. Medrano, Repression of TGF-β signaling by the oncogenic protein SKI in human melanomas: consequences for proliferation, survival, and metastasis, Oncogene 22 (20) (2003) 3123–3129, https://doi.org/10.1038/sj.onc.1206452.
[61] J.A. Reed, E. Bales, W. Xu, N.A. Okan, D. Bandyopadhyay, E.E. Medrano, Cytoplasmic localization of the oncogenic protein Ski in human cutaneous melanomas in vivo: functional implications for transforming growth factor beta signaling, Cancer Res. 61 (22) (2001) 8074–8078.
[62] M.J. Kruhlak, M.J. Hendzel, W. Fischle, N.R. Bertos, S. Hameed, X.J. Yang, D.P. Bazett-Jones, Regulation of global acetylation in mitosis through loss of histone acetyltransferases and deacetylases from chromatin, J. Biol. Chem. 276 (41) (2001) 38307–38319, https://doi.org/10.1074/jbc.M100290200.
[63] F. Fuks, W.A. Burgers, A. Brehm, L. Hughes-Davies, T. Kouzarides, DNA methyltransferase Dnmt1 associates with histone deacetylase activity, Nat. Genet. 24 (1) (2000) 88–91, https://doi.org/10.1038/71750.
[64] S. Ishii, Y. Kurasawa, J. Wong, L. Yu-Lee, Histone deacetylase 3 localizes to the mitotic spindle and is required for kinetochore-microtubule attachment, Proc. Natl. Acad of Sci. 105 (11) (2008) 4179–4184, https://doi.org/10.1073/pnas.0710140105.
[65] Y. Li, G.D. Kao, B. Garcia, J. Shabanowitz, D. Hunt, J. Qin, C. Phelan, M.a. Lazar, A novel histone deacetylase pathway regulates mitosis by modulating Aurora B kinase activity, Genes Dev. (2006) 2566–2579, https://doi.org/10.1101/gad.1455006.in.
[66] H.J. Shin, K.H. Baek, A.H. Jeon, S.J. Kim, K.L. Jang, Y.C. Sung, C.W. Lee, Inhibition of histone deacetylase activity increases chromosomal instability by the aberrant regulation

of mitotic checkpoint activation, Oncogene 22 (25) (2003) 3853–3858, https://doi.org/10.1038/sj.onc.1206502.
[67] F.E. Stevens, H. Beamish, R. Warrener, B. Gabrielli, Histone deacetylase inhibitors induce mitotic slippage, Oncogene 27 (10) (2008) 1345–1354, https://doi.org/10.1038/sj.onc.1210779.
[68] A. Taddei, C. Maison, D. Roche, G. Almouzni, Reversible disruption of pericentric heterochromatin and centromere function by inhibiting deacetylases, Nat. Cell Biol. 3 (2) (2001) 114–120.
[69] A.R. Robbins, S.a. Jablonski, T.J. Yen, K. Yoda, R. Robey, S. E. Bates, D.L. Sackett, Inhibitors of histone deacetylases alter kinetochore assembly by disrupting pericentromeric heterochromatin, Cell Cycle 4 (5) (2005) 717–726, https://doi.org/10.4161/cc.4.5.1690.
[70] J. Yang, X. Zhang, Y. Li, Y. Liu, Downregulation of Smad transcriptional corepressors SnoN and Ski in the fibrotic kidney: an amplification mechanism for TGF-β1 signaling, J. Am. Soc. Nephrol. 14 (12) (2003) 3167.3177, https://doi.org/10.1097/01.ASN.0000099373.33259.B2.
[71] H. Fukasawa, T. Yamamoto, A. Togawa, N. Ohashi, Y. Fujigaki, T. Oda, A. Hishida, Ubiquitin-dependent degradation of SnoN and Ski is increased in renal fibrosis induced by obstructive injury, Kidney Inter. 69 (10) (2006) 1733–1740, https://doi.org/10.1038/sj.ki.5000261.
[72] P. Li, P. Liu, R. Xiong, X. Chen, Y. Zhao, W. Lu, X. Liu, Y. Ning, et al., Ski a modulator of wound healing and scar formation in the rat skin and rabbit ear, J. Pathol. 223 (5) (2011) 659–671.
[73] J.H. Li, X.R. Huang, H.-J. Zhu, R. Johnson, H.Y. Lan, Role of TGF-beta signaling in extracellular matrix production under high glucose conditions, Kidney Int. 63 (6) (2003) 2010–2019, https://doi.org/10.1046/j.1523-1755.2003.00016.x.
[74] Y. Kanamaru, A. Nakao, Y. Tanaka, Y. Inagaki, H. Ushio, I. Shirato, Y. Tomino, Involvement of p300 in TGF-beta/Smad-pathway-mediated alpha2(I) collagen expression in mouse mesangial cells, Neph. Exper. Nephr. 95 (1) (2003) e36–e42, https://doi.org/10.1159/000073022.
[75] A.C. Poncelet, H.W. Schnaper, Sp1 and Smad proteins cooperate to mediate transforming growth factor-β1 induced α2(I) collagen expression in human glomerular mesangial cells, J. Biol. Chem. 276 (10) (2001) 6983–6992, https://doi.org/10.1074/jbc.M00644220.
[76] A. Bulut-Karslioglu, V. Perrera, M. Scaranaro, I.A. de la Rosa-Velazquez, S. van de Nobelen, N. Shukeir, J. Popow, B. Gerle, et al., A transcription factor-based mechanism for mouse heterochromatin formation, Nat. Struct. Mol. Biol. 19 (10) (2012) 1023–1030, https://doi.org/10.1038/nsmb.2382.
[77] Y. Liu, B. Pelham-Webb, D.C. Di Giammartino, J. Li, D. Kim, K. Kita, N. Saiz, V. Garg, et al., Widespread mitotic bookmarking by histone marks and transcription factors in pluripotent stem cells, Cell Rep. 19 (7) (2017) 1283–1293, https://doi.org/10.1016/j.celrep.2017.04.067.
[78] T. Fujita, M.W. Epperly, H. Zou, J.S. Greenberger, Y. Wan, Regulation of the anaphase-promoting complex-separase cascade by transforming growth factor-beta modulates mitotic progression in bone marrow stromal cells, Mol. Biol. Cell 19 (2008) 5446–5455, https://doi.org/10.1091/mbc.E08-03-0289.
[79] A. Zieba, K. Pardali, O. Söderberg, L. Lindbom, E. Nyström, A. Moustakas, C. Heldin, U. Landegren, Intercellular variation in signaling through the TGF-β pathway and its relation to cell density and cell cycle phase, Mol. Cell. Prot.: MCP 11 (7) (2012) M111, 013482 https://doi.org/10.1074/mcp.M111.013482.
[80] S.K. Zaidi, J.A. Nickerson, A.N. Imbalzano, J.B. Lian, J.L. Stein, G.S. Stein, Mitotic gene bookmarking: an epigenetic program to maintain normal and cancer phenotypes, Mol. Cancer Res. 16 (11) (2018) 1617–1624, https://doi.org/10.1158/1541-7786.mcr-18-0415.
[81] G. zhi Qu, P.E. Grundy, A. Narayan, M. Ehrlich, Frequent hypomethylation in Wilms tumors of pericentromeric DNA in chromosomes 1 and 16, Cancer Genet. Cytogenet. 4608 (98) (1999) 143–145, https://doi.org/10.1016/S0165-4608(98)00143-5.
[82] B. Cadieux, T.T. Ching, S.R. VandenBerg, J.F. Costello, Genome-wide hypomethylation in human glioblastomas associated with specific copy number alteration, methylenetetrahydrofolate reductase allele status, and increased proliferation, Cancer Res. 66 (17) (2006) 8469–8476, https://doi.org/10.1158/0008-5472.CAN-06-1547.
[83] H. Tsuda, T. Takarabe, Y. Kanai, T. Fukutomi, S. Hirohashi, Correlation of DNA hypomethylation at pericentromeric heterochromatin regions of chromosomes 16 and 1 with histological features and chromosomal abnormalities of human breast carcinomas, Am. J. Pathol. 9440 (10) (2002) 64246–64250, https://doi.org/10.1016/S0002-9440(10)64246-0.
[84] A. Narayan, W. Ji, X.Y. Zhang, A. Marrogi, J.R. Graff, S.B. Baylin, M. Ehrlich, Hypomethylation of pericentromeric DNA in breast adenocarcinomas, Int. J. Cancer 77 (6) (1998) 833–838, https://doi.org/10.1002/(SICI)1097-0215(19980911)77:6<833::AID-IJC6>3.0.CO;2-V.
[85] M. Lachner, D. O'Carroll, S. Rea, K. Mechtler, T. Jenuwein, Methylation of histone H3 lysine 9 creates a binding site for HP1 proteins, Nature 410 (6824) (2001) 116–120, https://doi.org/10.1038/35065132.
[86] I. Kuznetsova, O. Podgornaya, M.A. Ferguson-Smith, High-resolution organization of mouse centromeric and pericentromeric DNA, Cytogen. Genome Res. 112 (3–4) (2006) 248–255, https://doi.org/10.1159/000089878.
[87] B. Lehnertz, Y. Ueda, A.a.H.a. Derijck, U. Braunschweig, L. Perez-Burgos, S. Kubicek, T. Chen, E. Li, et al., Suv39h-mediated histone H3 lysine 9 methylation directs DNA methylation to major satellite repeats at pericentric heterochromatin, Curr. Biol. 13 (14) (2003) 1192–1200, https://doi.org/10.1016/S0960-9822(03)00432-9.
[88] B. Al-Sady, H.D. Madhani, G.J. Narlikar, Division of labor between the chromodomains of HP1 and Suv39 methylase enables coordination of heterochromatin spread, Mol. Cell 51 (1) (2013) 80–91, https://doi.org/10.1016/j.molcel.2013.06.013.
[89] M.R. Motamedi, E.J.E. Hong, X. Li, S. Gerber, C. Denison, S. Gygi, D. Moazed, HP1 proteins form distinct complexes and mediate heterochromatic gene silencing by nonoverlapping mechanisms, Mol. Cell 32 (6) (2008) 778–790, https://doi.org/10.1016/j.molcel.2008.10.026.
[90] N. Saksouk, T.K. Barth, C. Ziegler-Birling, N. Olova, A. Nowak, E. Rey, J. Mateos-Langerak, S. Urbach, et al., Redundant mechanisms to form silent chromatin at pericentromeric regions rely on BEND3 and DNA methylation, Mol. Cell 56 (4) (2014) 580–594, https://doi.org/10.1016/j.molcel.2014.10.001.
[91] R.B. Slee, C.M. Steiner, B.S. Herbert, G.H. Vance, R.J. Hickey, T. Schwarz, B.R. Grimes, Cancer-associated alteration of pericentromeric heterochromatin may contribute to chromosome instability, Oncogene 31 (27) (2012) 3244–3253, https://doi.org/10.1038/onc.2011.502.

[92] C. Gurrion, M. Uriostegui, M. Zurita, Heterochromatin reduction correlates with the increase of the KDM4B and KDM6A demethylases and the expression of pericentromeric DNA during the acquisition of a transformed phenotype, J. Cancer 8 (14) (2017) 2866–2875, https://doi.org/10.7150/jca.19477.

[93] G. Almouzni, A.V. Probst, Heterochromatin maintenance and establishment: lessons from the mouse pericentromere, Nucleus 2 (5) (2011) 332–338, https://doi.org/10.4161/nucl.2.5.17707.

[94] Y. Yamagishi, T. Honda, Y. Tanno, Y. Watanabe, Two histone marks establish the inner centromere and chromosome bi-orientation, Science 330 (6001) (2010) 239–243, https://doi.org/10.1126/science.1194498.

[95] M. Berk, S.Y. Desai, H.C. Heyman, C. Colmenares, Mice lacking the ski proto-oncogene have defects in neurulation, craniofacial patterning, and skeletal muscle development, Genes Dev. 11 (16) (1997) 2029–2039, https://doi.org/10.1101/gad.11.16.2029.

[96] P. Jeppesen, Immunofluorescence in cytogenetic analysis: method and applications, Genet. Mol. Biol. 23 (4) (2000) 1003–1014, https://doi.org/10.1590/S1415-47572000000400059.

[97] J.M. Vaquerizas, J. Dopazo, R. DÃaz-Uriarte, DNMAD: web-based diagnosis and normalization for microarray data, Bioinformatics 20 (18) (2004) 3656–3658, https://doi.org/10.1093/bioinformatics/bth401.

[98] A. Alibés, P. Yankilevich, A. Cañada, R. Díaz-Uriarte, IDconverter and IDClight: conversion and annotation of gene and protein IDs, BMC Bioinformatics 8 (2007) 9, https://doi.org/10.1186/1471-2105-8-9.

[99] A.I. Saeed, V. Sharov, J. White, J. Li, W. Liang, N. Bhagabati, J. Braisted, M. Klapa, et al., TM4: A free, open-source system for microarray data management and analysis, BioTechniques 34 (2003) 374–378https://doi.org/12613259.